



# Compressed earth blocks stabilized with glass waste and fly ash activated with a recycled alkaline cleaning solution

Jhonathan Rivera<sup>a</sup>, João Coelho<sup>b</sup>, Rui Silva<sup>c</sup>, Tiago Miranda<sup>d</sup>, Fernando Castro<sup>e</sup>, Nuno Cristelo<sup>a,\*</sup>

<sup>a</sup> CQ-VR, Department of Engineering, University of Trás-os-Montes e Alto Douro, Quinta de Prados, 5000-801, Vila Real, Portugal

<sup>b</sup> Department of Civil Engineering, University of Minho, 4800-058, Guimarães, Portugal

<sup>c</sup> ISE, Department of Civil Engineering, University of Minho, 4800-058, Guimarães, Portugal

<sup>d</sup> ISE, Institute of Science and Innovation for Bio-Sustainability (IB-S), Department of Civil Engineering, University of Minho, 4800-058, Guimarães, Portugal

<sup>e</sup> W2V, Department of Mechanical Engineering, University of Minho, 4800-058, Guimarães, Portugal



## ARTICLE INFO

### Article history:

Received 22 January 2020

Received in revised form

17 October 2020

Accepted 20 October 2020

Available online 23 October 2020

Handling editor: Prof. Jiri Jaromir Klemes

### Keywords:

Alkali activated cements

Sustainability

Earth construction

Soil stabilisation

Glass waste

## ABSTRACT

Sustainable alternatives are increasingly demanded as a sound response, from the construction industry, to the worldwide growing concerns with the environment. Such effort is justifiable by the degree of the contribution of this human activity to the problem, and it has thus propelled the development of a major trend in terms of funded research. The study reported in this paper focused on the physical-mechanical properties of compacted earth blocks formed by a common Portuguese silty clay (as the mineral skeleton), stabilized with a sustainable alkali activated cement exclusively produced from wastes and residues, including coal fly ash and glass waste, in a 50/50 wt ratio combination, and activated with an alkaline solution from the aluminium industry, using activator/precursor weight ratios of 0.50, 0.57 and 0.75. After optimising the alkaline activated cement (AAC), the AAC/Soil blocks were fabricated, using the response surface method to define their composition based on curing periods of 28 and 180 days at controlled ambient temperature. Uniaxial compressive strength (UCS) and several durability tests were performed, and the material was characterised using FTIR and SEM. The results evidenced the effectiveness of the alkaline cementing agent in forming a binding matrix for the soil particles. An average compressive strength of 17.23 MPa, in unsaturated conditions, was obtained for the blocks. The newly formed soil-binder structure was very capable to withstand wetting and drying cycles, ice-thaw cycles and erosion. The microstructure of the material was further analysed, using scanning electron microscopy and energy dispersive spectroscopy. The results demonstrated the real possibility of using this type of cement as a viable alternative to traditional soil stabilisation binders used in earth construction.

© 2020 Elsevier Ltd. All rights reserved.

## 1. Introduction

For millennia, compacted earth has been used all over the world, mostly for housing construction, and focusing on two techniques, known as “rammed earth” and “adobe” (Fernandes et al., 2019; Houben and Guillaud, 1994; Schroeder, 2016a, 2016b). Rammed earth is a thick wall of soil rammed inside a wooden formwork, while adobe is formed by blocks of compressed soil, usually slightly

larger than a clay brick, they may or may not include reinforcing fibres. Compacted earth blocks (CEB) are considered an evolution from adobe (Pacheco-Torgal and Jalali, 2012), since the manufacturing follows the same principle, only the compaction process has been improved and, additionally, chemical stabilisation is applied, thus improving mechanical properties and durability. The compaction technique has also evolved, from the appearance of the first CINVA-RAM (developed by Raul Ramirez in the Centro Interamericano Experimental y de Adiestramiento en Vivienda – CINVA) compactor machine, to the current use of hydraulic presses, capable of significantly improving the geometry and material properties of the CEB (Silva et al., 2015).

The chemical stabilisation of soils to manufacture CEB is

\* Corresponding author.

E-mail addresses: [jhonathan@utad.pt](mailto:jhonathan@utad.pt) (J. Rivera), [id7225@uminho.com](mailto:id7225@uminho.com) (J. Coelho), [ruijsilva@civil.uminho.com](mailto:ruijsilva@civil.uminho.com) (R. Silva), [tmiranda@civil.uminho.com](mailto:tmiranda@civil.uminho.com) (T. Miranda), [fcastro@w2v.pt](mailto:fcastro@w2v.pt) (F. Castro), [ncristel@utad.pt](mailto:ncristel@utad.pt) (N. Cristelo).

traditionally done with Portland cement (OPC) or lime. However, in some cases, these traditional cements are not a viable solution due to the financial cost of the material, if high cement contents are required to obtain adequate properties. Therefore, it is justifiable to research and develop alternative binders, with a clear capacity to contribute to a more environmentally friendly material. In that context, different families of binders, based on industrial wastes or by-products, are gaining rapid acceptance (Miranda et al., 2020; Saeli et al., 2019, 2020; Shoukry, 2019; Singh et al., 2020), thus becoming ideal for this particular application. From a relatively large pool of possibilities, fly ash (FA) is a clear target, due to its extensive research in the last 20 years, which includes applications as a soil stabilizer and as a precursor in alkaline activation reactions. This residue from the combustion of coal, in thermoelectric powerplants, can act as a soil filler, reducing the settlement of the resulting material, or can also be used together with a source of calcium, taking advantage of its pozzolanic properties (Horpibulsuk et al., 2009; Siddiqua and Barreto, 2018).

Slags are also one of the most used wastes in this type of applications, and especially ground granulated blast furnace slags (GGBS), because of its high content in calcium oxides and hydraulic character, that makes them very similar to OPC. Oti et al. (2009a, 2009b) used mixtures of GGBS and quick lime or hydraulic lime to stabilize a clayey soil, which was then compacted with a hydraulic press to produce CEB. The GGBS/lime binder improved compressive strength and especially the durability, in terms of ice/thaw cycles. Mixtures of GGBS and OPC showed less effective results, which was attributed to the increased cationic exchange capacity between the soil and the lime-based binder. In addition to FA and GGBS, it is also worth mentioning the successful use, as chemical stabilizers for the manufacture of CEB, of ashes from sugarcane bagasse and marble stone cutting muds. El-Mahllawy et al. (2018) and Lima et al. (2012) mixed this type of waste with OPC and lime, in varied percentages, effectively improving properties such as compressive strength and absorption of the CEB.

Glass wastes (GW) are used, since the 1970s, in the manufacture of baked bricks. Due to its very specific composition, they function as a melting material in the sintering process of clay minerals (Hwang et al., 2006; Zhang et al., 2018). However, the use of glass waste as a chemical stabilizer in the manufacture of CEB is not possible, because it is completely inert if not in contact with a strong alkaline substance or a high acidic medium. Therefore, in geotechnics, they are used mostly as a filler material, as a plasticity modifier or to increase the internal friction angle of clay soil particles (Olufowobi et al., 2014). In order to improve and use glass wastes as cementing materials, methods such as alkaline activation are showing significant potential, mostly due to the capacity of the alkaline activators, mainly alkali metal salts, to dissolve the previously pulverized glass. Several authors (Avila-López et al., 2015; Espinoza and Escalante García, 1970; Lin et al., 2012; Novais et al., 2016; Pascual et al., 2014; Rivera et al., 2018) have successfully used alkaline activated glass waste as a cementitious material in various applications, demonstrating that pulverized glass waste can be an alternative to traditional Portland cements, either when used as the sole precursor or mixed with other aluminosilicate-rich precursors.

The alkaline activation technique is no stranger to the development of masonry elements made of raw earth. This technique, combined with precursor residues or commercial aluminosilicates, such as metakaolin, have been used to chemically stabilize soils for subsequent compaction and manufacture of CEB. Very interesting results have been obtained, using different types of precursor, either fly ash (Leitão et al., 2017; Rivera et al., 2020; Silva et al., 2015), metakaolin (Omar Sore et al., 2018) or blast furnace slag (Preethi and Venkatarama Reddy, 2020; Sekhar and Nayak, 2018);

or even using soil-substitute wastes, as successively shown by Shaker et al. (2020), whom tested palm oil residues as a substitute for the soil matrix. All these studies reflect the capacity of this type of sustainable binders to greatly improve the mechanical properties, durability and water stability of the compacted blocks, developing performances comparable to the CEBs stabilized with OPC. Furthermore, a step forward was already given towards the implementation of alternative, more environmentally friendly activators, with an optimised incorporated energy, with the purpose of producing masonry with a very low carbon footprint. Recent research (Cristelo et al., 2019; Fernández-Jiménez et al., 2017) has shown that the use of glass waste, combined with precursors like fly ash and aluminium anodizing sludge, activated with a recycled alkaline cleaning solution, can originate a sustainable alkaline cement. The sustainability of the alkaline cement - based CEBs was also shown by several authors, whom developed comparative studies, including technical performance (Shaker et al., 2020), but also life-cycle analysis, between CEBs produced with Portland cement and alkaline binders (Narayanaswamy et al., 2020).

In the present work, the physical-mechanical characterization of chemically stabilized CEB was carried out, integrating various types of industrial waste into the soil stabilisation process and manufacturing of the CEB, with the intention of replacing traditional precursors, such as blast furnace slag or metakaolin, and alkaline activators such as hydroxides or silicates. The main novelty, relatively to previous studies, is based on the sole use of wastes to produce the stabilizing binder. This is usually not the case, since commercial reagents are the most common activators to date.

## 2. Materials and methods

### 2.1. Materials

The soil was collected in the area of Chaves, a city in the Northern Region of Portugal famous for its clay bricks and roof tiles industry, due to the quality of the clayey soil. The fly ash was generated by the Portuguese thermo-electric powerplant of Pego. According to ASTM C618 (2012), it was classified as a class F. The glass waste powder results from the production of optical lenses at the Portuguese company POLO. The chemical composition of the soil and precursors is presented in Table 1, obtained by x-ray fluorescence with a PHILLIPS PW-1004 spectrometer.

As stated above, the use of wastes as activators, in the production of alkaline cements, is of critical importance, since the current option is to use commercial reagents, with their heavy toll in terms of CO<sub>2</sub> production and economical cost. With this concern in mind, a recycled cleaning solution was considered as the alkaline activator. It has a high pH (an absolutely decisive factor in alkaline activation), between 12 and 14, with an approximate density of 1.3 g/cm<sup>3</sup>. It underwent a homogenization process before collection

**Table 1**  
Chemical composition of the Fly ash, Soil and Waste glass (%w).

Element (oxides)	Fly ash	Soil	Waste glass
SiO <sub>2</sub>	56.11	61.74	58.37
Al <sub>2</sub> O <sub>3</sub>	21.44	23.27	3.94
Fe <sub>2</sub> O <sub>3</sub>	8.20	5.68	0.15
CaO	1.31	0.33	6.13
MgO	1.46	1.65	0.49
TiO <sub>2</sub>	1.15	0.08	—
MnO	0.07	0.89	2.73
Na <sub>2</sub> O	1.12	0.58	8.75
K <sub>2</sub> O	2.81	5.12	4.66
P <sub>2</sub> O <sub>5</sub>	0.29	0.09	5.07
LOI	5.05	0.33	1.85

**Table 2**  
Elemental composition of the cleaning solution.

Al <sub>2</sub> O <sub>3</sub>	Na <sub>2</sub> O	SO <sub>3</sub>	H <sub>2</sub> O	pH	<sup>a</sup> [OH] <sup>-</sup>	Density (g/cm <sup>3</sup> )
7.14	12.13	1.18	79.5	12–14	5.3	1.30

<sup>a</sup> Acid-base reaction with 5 N HCL (Panrea S.A.).

from the storage tanks. Table 2 shows its elementary composition, determined by Inductively Coupled Plasma Atomic Emission Spectrometer (ICP-AES), with plasma power of 1.4 kW, plasma gas flow of 15.00 l/min and gas nebulizer flow of 0.85 l/min, with a reading time of 5s.

Fig. 1 shows the particle size distribution of the soil and both precursors. The curves were obtained by laser diffraction, using a Sympatec Helos BF particle size analyser, with a measuring range between 0.9 μm and 175 μm. The particle size below 45 μm was 75.6, 81.3 and 99.2% for fly ash, soil and glass waste, respectively.

The mineralogical composition of the soil and precursors and the soil was determined using X-ray diffraction (XRD), with a PANalytical X'Pert Pro MPD, with CuKα radiation at 40Kev and 30 mA, equipped with a detector X'Celerator and a secondary monochromator. The diffractograms are presented in Fig. 2. The glass residue is a highly amorphous material, as evidenced by the large halo between the 17°(2θ) to 37°(2θ) angles. The fly ash is a semi-crystalline material, also with some amorphous content, represented by a smaller halo between angles 18°(2θ) and 32°(2θ). It is mineralogy composed essentially by quartz, mullite and hematite. As expected, the soil is a totally crystalline material, composed of several minerals such as quartz, kaolinite magnetite and albite.

## 2.2. Definition of the alkaline cement

Prior to the stabilisation of the soil, it was necessary to define the composition of the alkaline activated cement (AAC) that would be used as a binder. This AAC was prepared with the described cleaning solution (CS), which was used to activate the glass waste (GW) and the fly ash (FA), acting as the precursor, in a 50/50 wt ratio. The CS was added according with pre-defined activator/precursor weight ratios of 0.50, 0.57 and 0.75. The lowest of these values was defined based on the minimum workability requirements. The pastes were then moulded in 4 cm cubic specimens, which were cured at 50 °C and 10% relative humidity in a climatic chamber, for 7 days. Fig. 3 presents the uniaxial compressive strength (UCS) obtained by each of the AAC tested. The

highest UCS (11.6 MPa) was obtained with the lower activator/precursor ratio of 0.50.

## 2.3. Definition of the AAC/soil composition

To define the most adequate activator content, in terms of dry density, a Standard Proctor test was carried out based on the methodology proposed by the EN13286-42 (2004), using the AAC with an activator/precursor ratio of 0.50 as a starting point. The test was performed with 3 layers and 12 blows per layer, on pastes with a precursor/soil weight ratio of 30/70. A curve was obtained (Fig. 4) by adding more or less activator to the solids (precursor + soil), from which the maximum dry density and optimum moisture content were identified as 1.77 g/cm<sup>3</sup> and 17%, respectively.

However, when the CEB was compacted, significant expansion was registered, which was attributed to excessive moisture. This is a negative consequence of the application of the Proctor test concept to stabilized soils, which is, based on the authors experience, magnified when the binder is not only in development, but it also comprises further variables, in terms of preparation and setting behaviour, than conventional Portland cement. The Proctor test is heavily based on the accurate assessment of the water content. However, in this case, the liquid phase in the test is the activator, which, although with a significant percentage of water in its composition, includes also sodium, silicon and hydroxide ions, thus increasing the difficulty in quantifying the water used for the lubrication of the particles (traditional role of the water in the compaction of granular materials). Furthermore, part of this water evaporates due to the exothermic alkaline reactions. To overcome the described initial problems associated with the fabrication of the CEB, it was decided to further optimise the moisture content in the AAC/soil composition, using a value lower than 17% (determined by trial and error), without reducing the volumetric weight of 1.77 g/cm<sup>3</sup> obtained during the Proctor test. Maintain the volumetric weight while reducing the water (activator) content was only possible due to the higher energy that is possible to apply by the block compaction machine, compared with the dynamic energy transmitted by the Proctor hammer.

This experimental optimisation was design using the response surface methodology (RSM), which is, in essence, a mathematical model targeting the minimization of the experiments required to achieve a pre-determined information. It also allows a very effective data analysis and interpretation, including the inference of further results if different scenarios are developed. A Central Composite Design (CCD) was configured with the aim of finding a

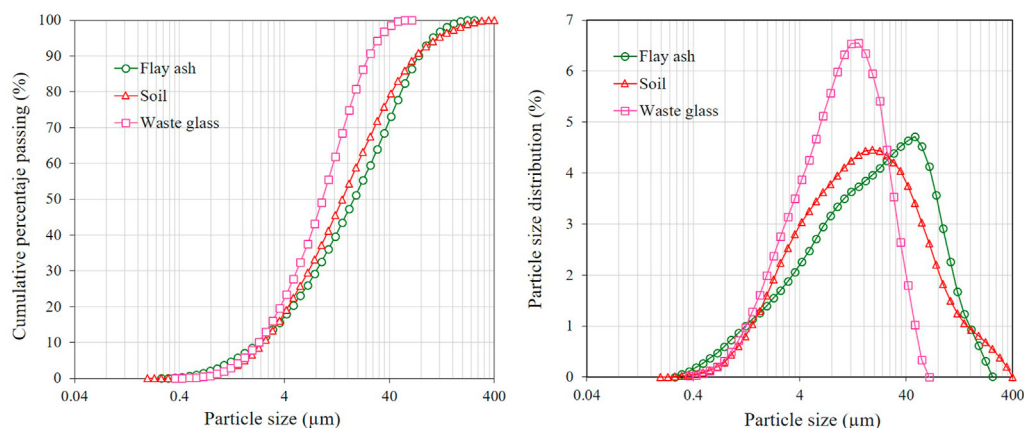


**Fig. 1.** Cumulative particle size and particle size distribution of the Fly ash, Soil and Waste glass.

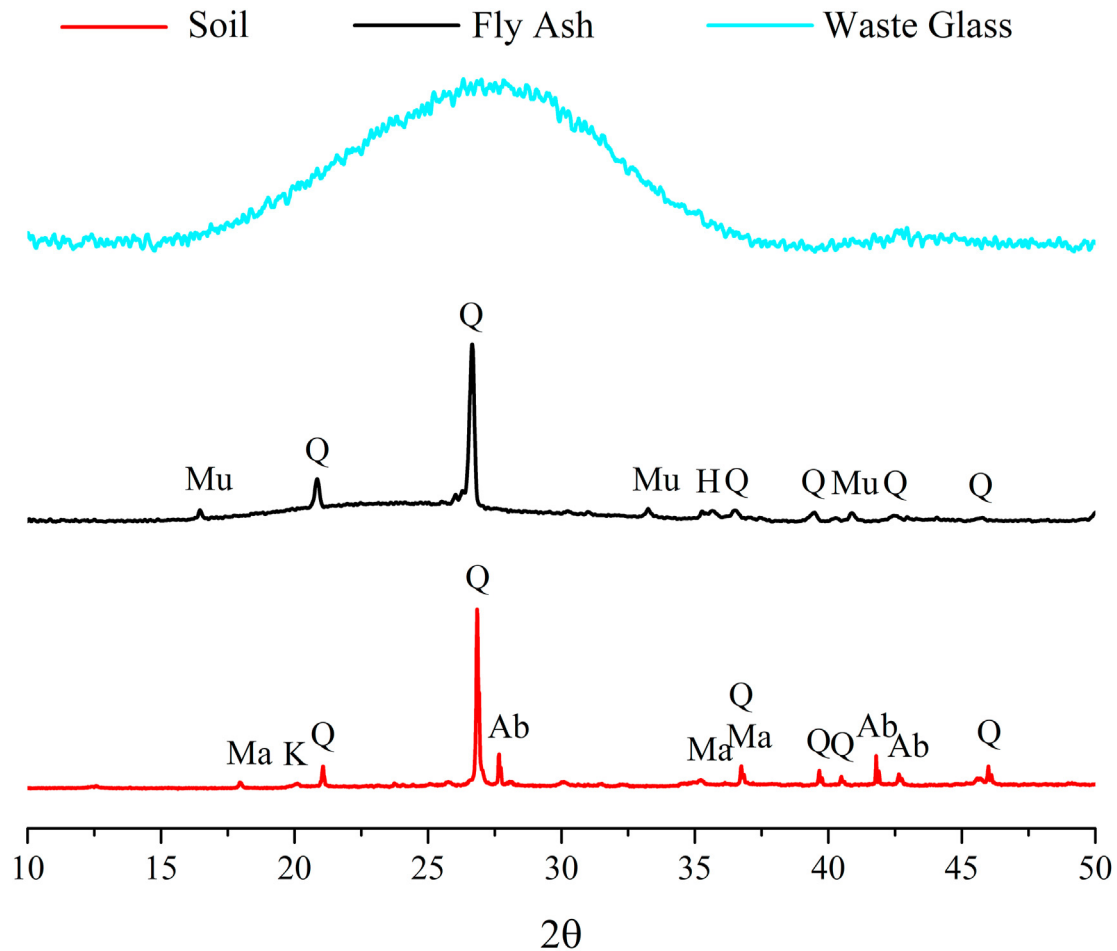


**Fig. 2.** XRD Pattern of the original materials (Mu = mullite,  $\text{Al}_6\text{Si}_2\text{O}_{13}$  PDF-079-1453; Q = quartz,  $\text{SiO}_2$  PDF-46-1045; H = hematite,  $\text{Fe}_2\text{O}_3$  PDF-33-664; K = kaolinite,  $\text{Al}_2\text{Si}_2\text{O}_5(\text{OH})_4$  PDF-14-164; Ma = magnetite,  $\text{Fe}_2\text{O}_4$  PDF-075-1610; Ab = albite,  $\text{NaAlSi}_3\text{O}_8$ ).

relation between the independent variables and the response variable (compressive strength) capable of maximize the latter (Montgomery and Runger, 2014), therefore defining the most effective AAC/soil combination. Table 3 presents the independent variables considered (i.e. soil/precursor and activator/solids weight ratios), as well as their respective range. The commercially available software *Minitab 17* was used which, based on the number of independent variables assumed, established a total of 13 random runs. The soil/precursor range was defined based on previous experience by the research team (Corrêa-Silva et al., 2019; Cristelo et al., 2018; Miranda et al., 2017; Rios et al., 2016); while the activator/solid range was defined after the maximum and minimum CS content in the paste that presented the most adequate workability. This range was on the 'dry side' of the Proctor curve, thus below the 17% humidity threshold that produced the expansion of the paste. The response variable was assessed through compressive strength tests on compacted specimens with 70 mm in diameter and 140 mm in height, cured at  $20 \pm 1^\circ\text{C}$  for 28 and 180 days.

The influence of each independent variable and the corresponding compressive strength is presented in Fig. 5. For the 28-day curing period, higher UCS were attained when the pastes showed the highest CS content, regardless of the precursor content; while for 180-day period the higher UCS was recorded when the CS and precursor contents simultaneously assumed their higher values. The final values of each independent variable, based on the

compressive strength data of 11.4 MPa (desirability of 0.82), obtained after 180 days (Fig. 5), were set at soil/precursor = 2.3 and activator/solids = 0.21.

#### 2.4. Fabrication of the compressed earth blocks

The CEB were fabricated with the optimised AAC-soil combination. The main steps towards the production of each block are presented in Fig. 6, and involve, after a thorough mixture of the soil with the binder, the filling of two simultaneous moulds, in a fully manually operated CEB machine, their subsequent compression and, finally, the curing and drying stage. Considering that the 180-day curing result was chosen as the reference, and to avoid such prolonged waiting, the CEBs were cured at  $85^\circ\text{C}$  for 20 h, to accelerate the dissolution stage and the production of binding gel (Bakharev, 2005; Criado et al., 2010; Fernández-Jiménez et al., 2006, 2008; Torres-Carrasco et al., 2014; Torres-Carrasco and Puertas, 2015).

The physical-mechanical characterization of the CEBs was carried out with compressive strength tests, water absorption tests, wetting-drying tests, ice-thawing tests and water erosion tests. Furthermore, the microstructural characterization of the AAC-soil was performed using Fourier Transform Infra-Red Spectroscopy (FTIR) and Scanning Electron Microscopy (SEM).

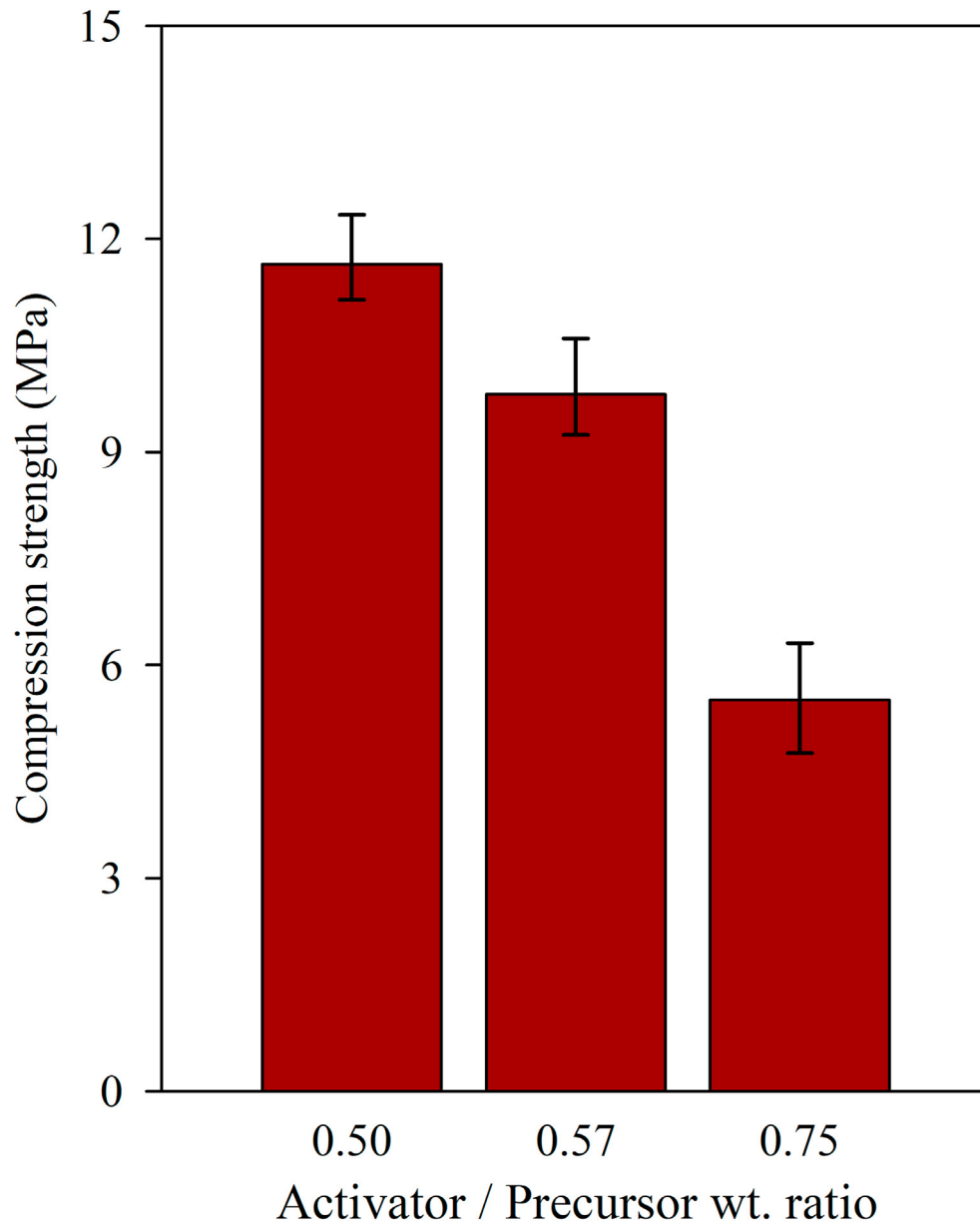


Fig. 3. Compressive strength, after 7 days curing, of the 50% FA + 50% GW precursor paste.

### 3. Results and discussion

#### 3.1. Mechanical performance of the CEBs

The compressive strength is mostly accepted as a universal property to determine the quality of the CEBs. In general, the compressive strength is related to the type of soil; type and amount of stabilizer; compaction pressure and process. Table 4 summarizes the compressive strength results performed on the CEBs in both dry and saturated conditions, together with the percentage of water absorption until saturation. Regarding the absorption values, the experimental procedure described in the UNE 41410 (2008) standard, specifically prepared for CEB testing, was followed. It consists of submerging the bottom 1 cm of a dry CEB in potable water, while sealing the lateral faces, thus forcing the water to move only upwards. The CEB is then weighted after periods of 5, 10, 15, 30 and 60 min; every hour after that until 7 h; and 24 and 48 h after the

start of the test. The absorbed water is then calculated using the dry mass as a reference.

The maximum compressive strength reached by the CEB (17.23 MPa) was significantly higher than the uniaxial compressive strength developed by the optimum AAC/soil formulation (11.4 MPa). Such increase, of more than 50%, is not attributed to the geometry differences between the two types of specimen, but mostly to the thermal curing that was implemented for the CEB, as well as to the different compositions (i.e. different soil/precursor ratio). According to some authors (Bakharev, 2005; Singh and Subramaniam, 2019) fly ash-based alkaline cements generate mechanical strength very slowly at room temperature. On the contrary, the dissolution of the amorphous phase of the fly ash is improved if the curing occurs under an increased temperature (Rivera et al., 2018; Torres-Carrasco and Puertas, 2015), generating aluminosilicate gel in shorter periods and, thus, increasing the strength development rate of the material (Ryu et al., 2012;



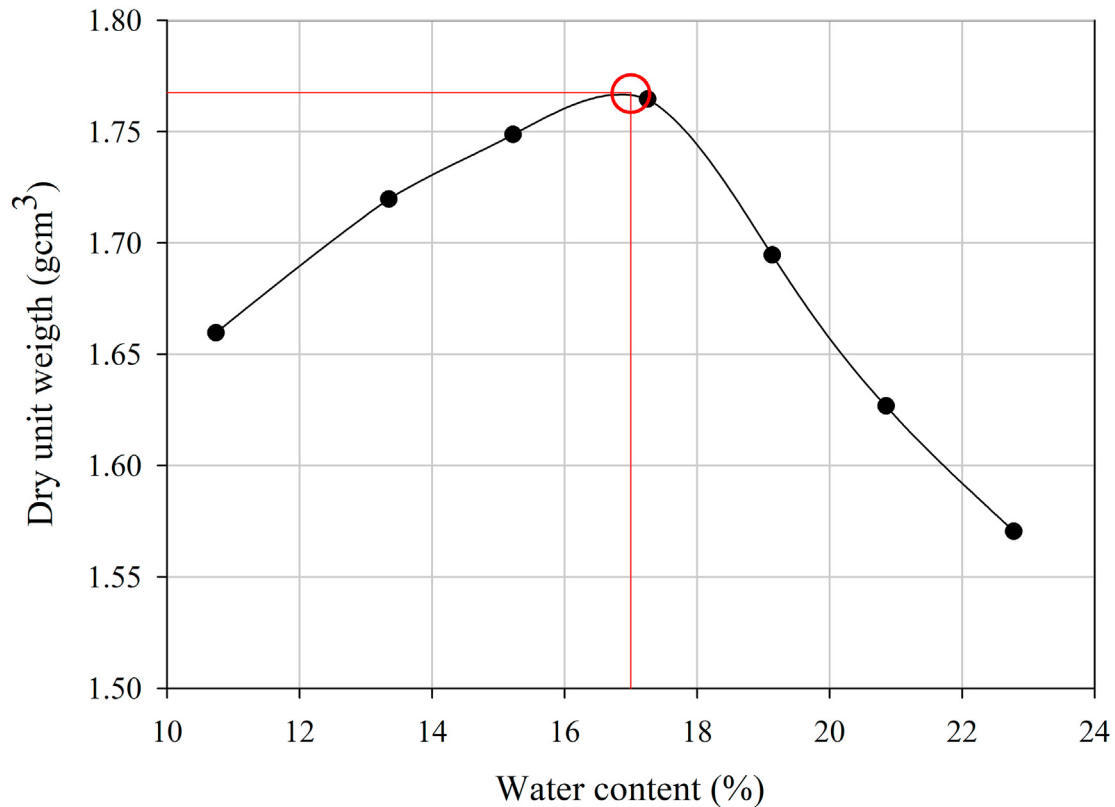


Fig. 4. Proctor test results for the stabilized soil, using the activator as the liquid phase and a precursor/soil weight ratio of 30/70.

**Table 3**

Definition of the independent variables and corresponding value range.

Variable	Level	Value
Activator/Solids	Lower (–)	0.12
	Upper (+)	0.25
	Central Point	0.18
Soil/Precursor	Lower (–)	2.3
	Upper (+)	4.0
	Central Point	3.1

Šimonová et al., 2018; Singh and Subramaniam, 2019).

The UNE 41410 (2008) standard classifies the CEBs in three categories, according to its respective compressive strength: CEB1, CEB3 and CEB5. Each category corresponds to the minimum compressive strength of the CEB, e.g. category CEB5 corresponds to the blocks with a strength of at least 5 MPa. According to this standard, it is possible to classify the present CEB in the CEB5 category. ASTM C62-17 (2017) specifies the minimum requirements of solid masonry made of compacted clay or similar materials, sintered at high temperatures. Based on this standard, the CEB designed in this research can be classified as a 'MW' grade brick, with the advantage that in the manufacturing process of the block no high temperatures were used for sintering its components. This means that good mechanical properties were achieved with an amount of incorporated energy well below the energy required to fabricate a cooked brick, thus filling a decisive requisite if sustainable alternatives are ever to be fully adopted.

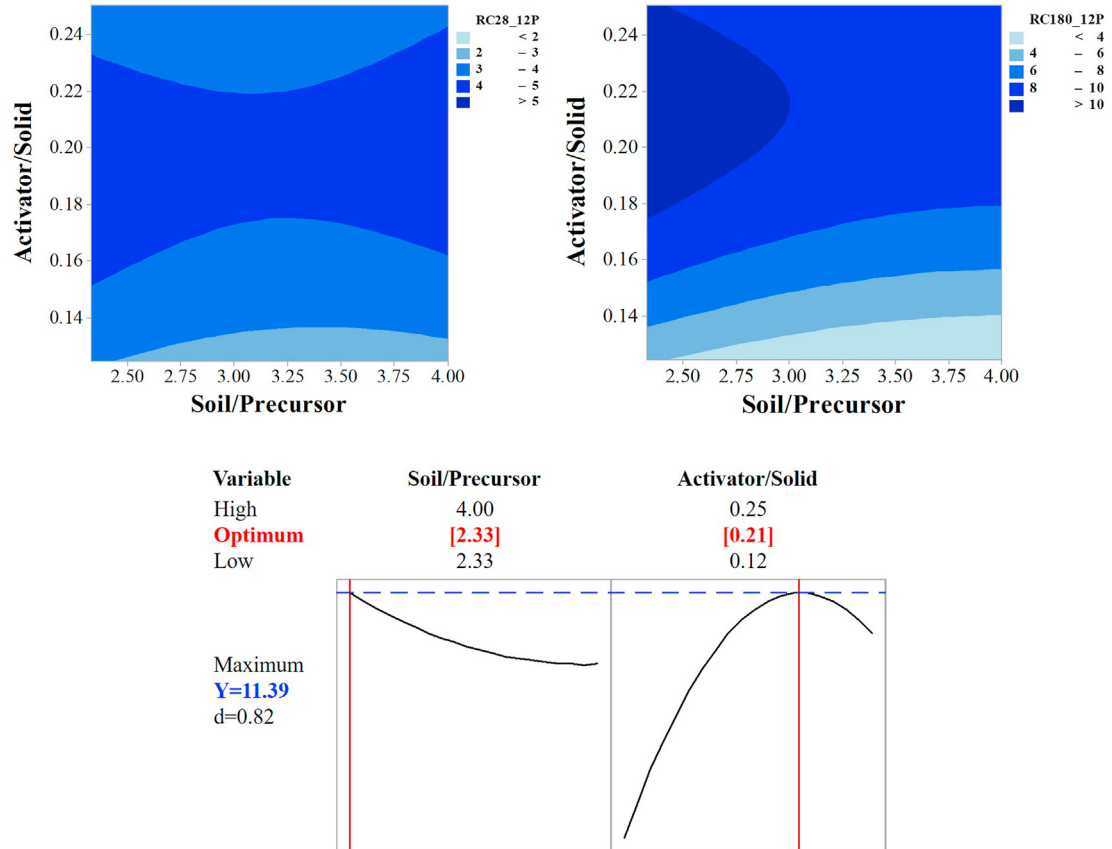
### 3.2. Durability tests

Fig. 7 shows images of the evolution of the wetting-drying test,

using a total of 7 blocks, following the contents of the UNE 41410 standard. This test requires two CEBs, using one only as a reference, while the bottom 1 cm of the other is submerged in water for 30s. This second CEB is then completely air dried, and its resulting physical state is thoroughly observed and compared with the intact CEB. This is repeated for a total of 6 cycles. After detailed visual inspection, no significant deterioration was observed after the planned 6 cycles of wetting-drying. This corroborates that the stabilisation of the soil and the cementation of its particles was very effective, to the point where the physical integrity of the blocks was not affected by the volume changes intentionally induced by the test.

The CEBs were submitted to ice-thaw tests, based on the methodology proposed by the DIN 18945-47 (2013) standard. The durability assessment of the blocks is particularly important since they mostly measure their longevity (Preethi and Venkatarama Reddy, 2020; Shakir et al., 2020). Moreover, sequential submission to freezing and thawing is one of the most aggressive environmental conditions for this class of compacted earth masonry elements. The humidity lodged in the structure of the compacted piece, at the time of the freezing, generates internal pressure in the pores due to the increase in volume of the frozen water, which can even cause a structural collapse (Jamshidi et al., 2016; Mak et al., 2016). Fig. 8 presents the temperature profile used during the test, comprising a total of 15 cycles. The exposed surface of the block was moistened and submitted to the temperature variations. At the end of the 15 cycles, no significant damage was observed, including gaps, cracks, fractures or delamination of the material, demonstrating that the structure of the stabilized CEB was strong enough to withstand the stresses caused by the internal pressure of the frozen water during the test.

The durability of the CEBs was also evaluated through their



**Fig. 5.** Contour diagrams showing the relation between the independent variables and the UCS after 28 days (left) and 180 days curing (right) on the AAC/soil (top); and optimised independent variables and resulting UCS and desirability values.

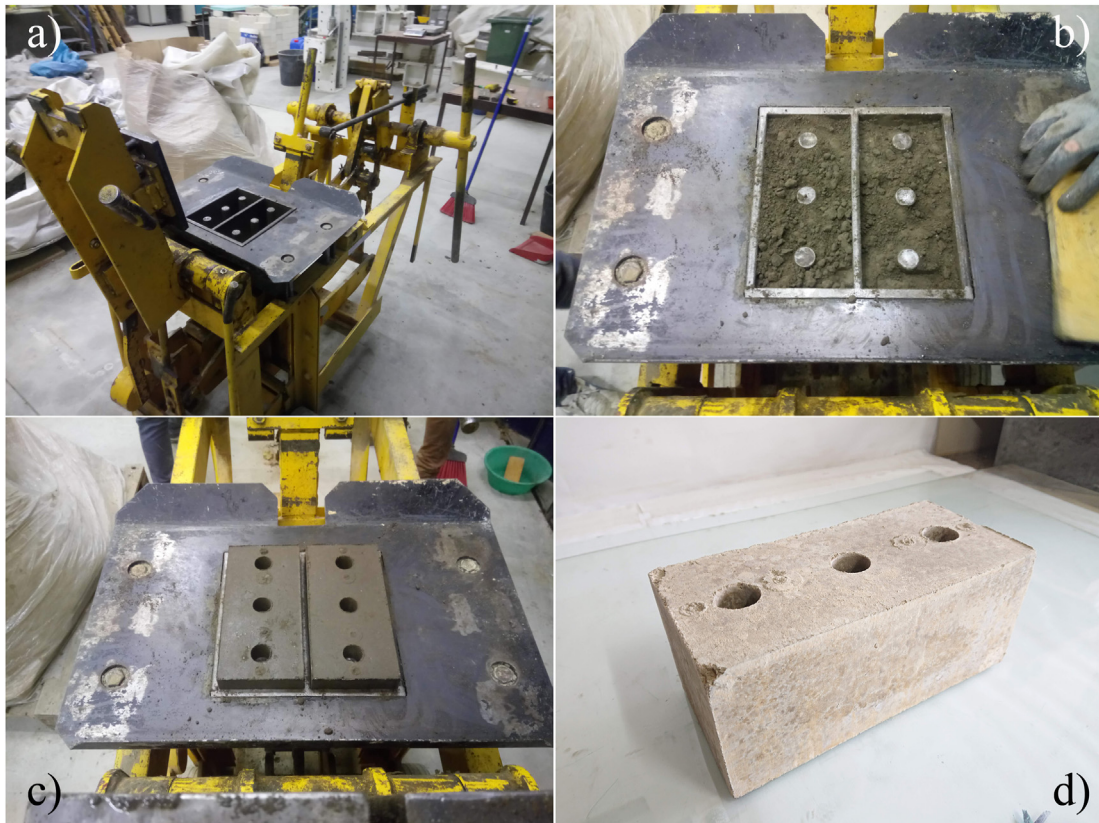


**Fig. 6.** Main steps in the fabrication process of the CEBs, including, after mixture of the soil with the alkaline cement, the filling of the moulds (a and b), the subsequent compression (c) and the curing and drying of the resulting blocks (d).

**Table 4**  
Compressive strength and water absorption of the CEBs (UNE 41410, 2008).

Property		Type of specimen	
		Unsaturated/Dry CEB	Saturated CEB
Compressive strength (MPa)	Average	17.23	7.45
	Range	14.94–19.39	6.35–9.29
	N° of specimens	4	4
Water absorption after 24 h (%)	Average	16.21	—
	Range	15.92–16.49	—
	N° of specimen	6	—

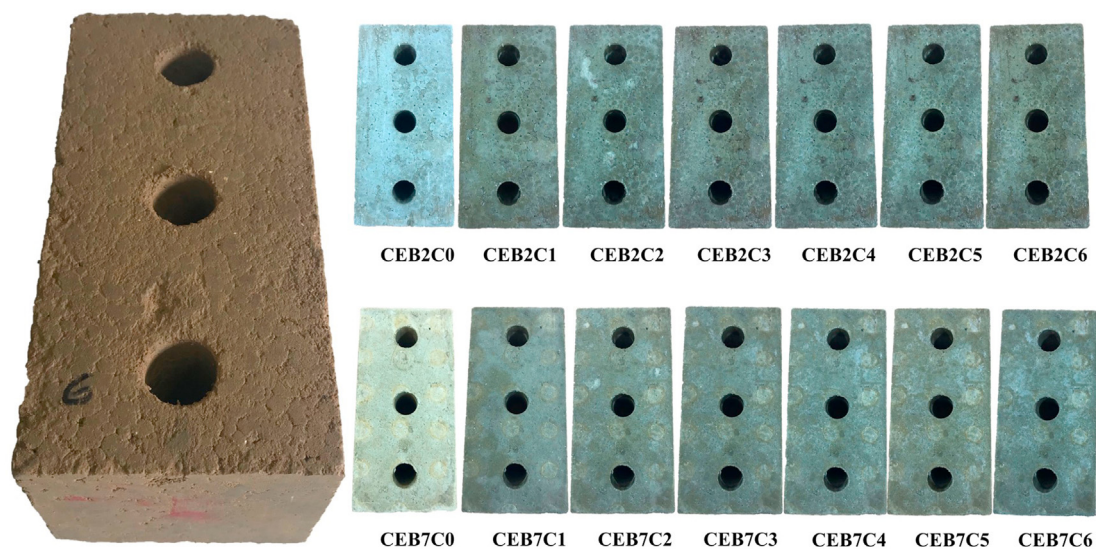


**Fig. 7.** Evolution of two different CEB specimens submitted to the wetting and drying durability test cycles.

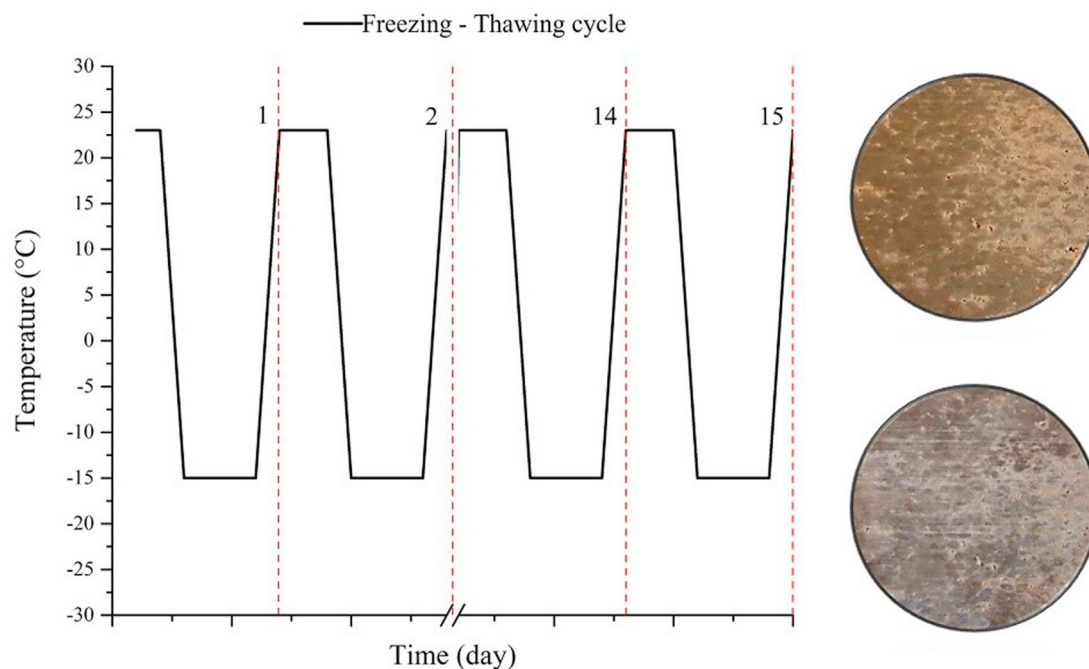


**Fig. 8.** Freeze-thaw temperature cycles.

resistance to water erosion, tested according to the Swinburne test (SAET), as established in the Spanish standard [UNE 41410 \(2008\)](#).

This test was specifically developed for earthen materials and simulates the accelerated erosion action of hitting rain. The test





Fig. 9. Swinburn test setup (a); surface of the CEB after exposure (b); water penetration depth (c).

Table 5

Results of the Swinburn test (CoV in brackets).

Specimen	Pitting depth (mm)	Moisture penetration depth (mm)
S1	0	9
S2	0	10
S3	0	8
Average	0	9 (16%)

setup consists of a deposit, elevated 1 m above the exposed surface of the CEB, which continuously drops water on the surface of the CEB from an outlet of 5 mm diameter, while keeping a constant water head of 0.5 m (Fig. 9a). The surface of the CEB is inclined  $27^\circ$  relatively to the horizontal plane. The water dropping lasts 10 min, after which the specimen is opened and the pitting depth caused by the water stream is measured, using a 3 mm diameter probe. According to the contents of the mentioned standard, the CEBs are suitable if the pitting depth is not higher than 10 mm.

The results of the three specimens tested are presented in Table 5. As can be seen in Fig. 9b, the water stream did not cause any surface degradation, meaning that the stabilisation solution used is highly effective in providing water erosion resistance to the CEBs. The moisture penetration depth was additionally measured, by breaking the specimens into 2 halves along the longitudinal section hit by the stream (Fig. 9b). An average value of 9 mm was observed, although all specimens showed some variation in the penetration depth (Fig. 9c), which was caused by the presence of some clogs formed during the mix located near the surface, facilitating the water intake.

The durability results showed that the material developed can withstand the requirements for this type of materials and construction products. This is very significant, as the durability of earth blocks is, at least, as relevant as their compressive strength, due to the particular applications (masonry) to which they are submitted during their service life.

### 3.3. FTIR

Fig. 10 shows the IR spectra of the raw material with which the CEBs were manufactured. The FA and WG residues have several signals in common – bands centred around  $455$ ,  $774$  and  $776\text{ cm}^{-1}$ , associated with Si–O (quartz) functional groups. The main band of the FA is located around  $1023\text{ cm}^{-1}$ , characteristic of Si–O–T (T = Al, Si) type links. This spectrum is typical of a material rich in aluminosilicates (Criado et al., 2007; Gao et al., 2014; Pánias et al., 2007; Rivera et al., 2019). The GW has a main band centred around  $959\text{ cm}^{-1}$ , and the signals located between  $950$  and  $1000\text{ cm}^{-1}$  are associated with vibration modes of Si–O–Na functional groups in condensed units of type Q2 and Q3 silicates, typical of a calcium sodium glass (Khalil et al., 2010; Rivera et al., 2018; Varma et al., 2009; Véron et al., 2013). The characteristic spectrum of the soil reveals signals at  $455\text{ cm}^{-1}$ ,  $748\text{ cm}^{-1}$  and  $998\text{ cm}^{-1}$  wave lengths, associated with vibration modes of Si–O–Si and Si–O functional groups (i.e. quartz). The band signal around  $529\text{ cm}^{-1}$  can be attributed to stretching vibrations of Fe–O, Fe<sub>2</sub>O<sub>3</sub> and Si–O–Al type bonds, while bands in the region  $850$ – $950\text{ cm}^{-1}$  are characteristic of O–H–Al type links, and the band identified at  $1633\text{ cm}^{-1}$  is attributed to bending vibration modes of O–H–O type bonds of water molecules (Kaufhold et al., 2012; Nayak and Singh, 2007; Saikia and Parthasarathy, 2010).

The cleaning solution, being a highly alkaline aqueous solution contaminated by the aluminium foundry industry, is basically composed by products from the reaction between caustic soda and aluminium waste. In its IR spectrum, a signal centred at  $527\text{ cm}^{-1}$  can be observed, attributed to non-condensed octahedral species of AlO<sub>6</sub> (these octahedral species can present signals between  $400$  and  $530\text{ cm}^{-1}$ ). The region between  $700$  and  $900\text{ cm}^{-1}$  is characteristic of AlO<sub>4</sub> tetrahedral species (Tarte, 1967). Therefore, it is not surprising that ionic species of Al(OH)<sup>−4</sup> aluminates in solution were identified in this same region. These aluminate species are predominant in pH values between 8 and 12, with vibrations of Al–OH type bonds (Li et al., 2014; MA et al., 2007). According to Ram (2001), the bands in the IR spectrum of the cleaning solution

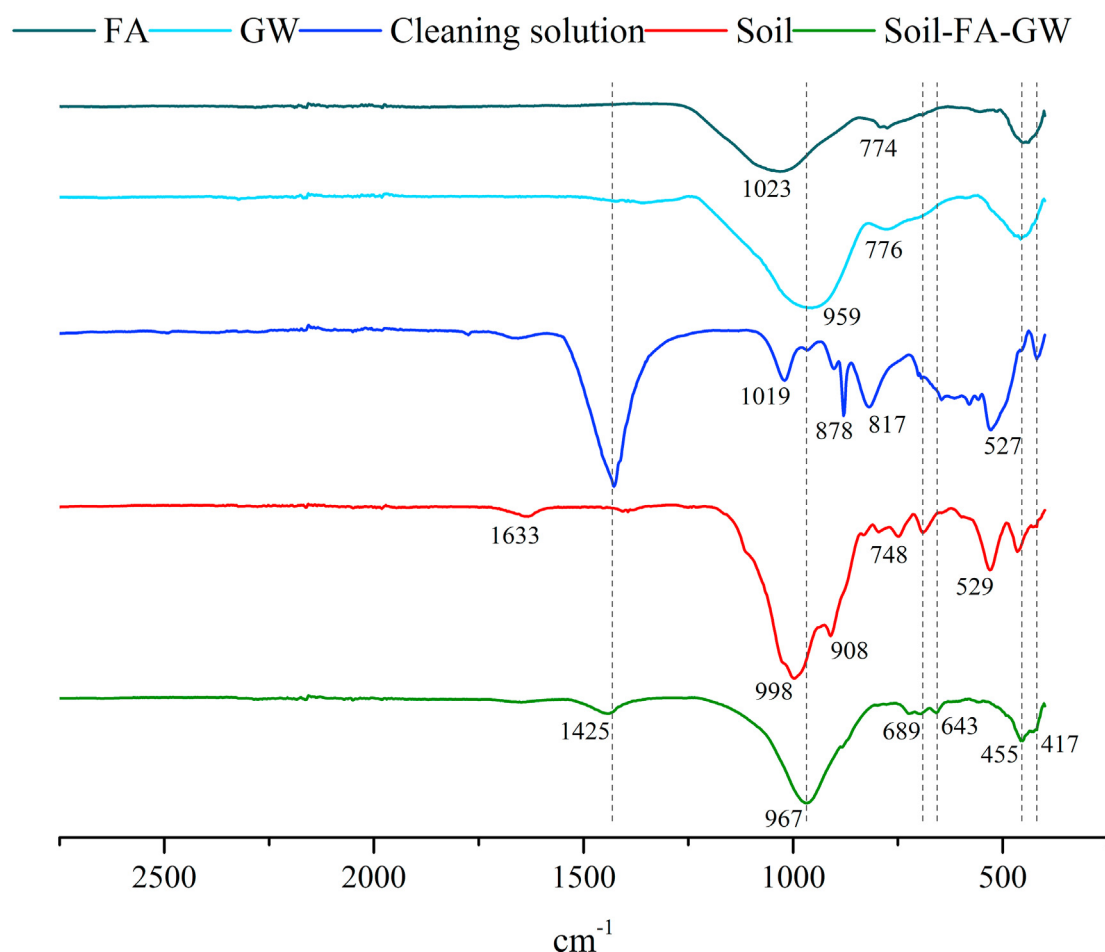


Fig. 10. FT-IR spectra of the original and stabilized materials.

around 1019 and 1420  $\text{cm}^{-1}$  could be considered as vibration signals of double bond stretching of  $\text{Al}=\text{O}$  amorphous compounds. In short, and as expected, signals of aluminate compounds and aluminium hydroxides were found in the spectrum of the cleaning solution.

When stabilizing the soil-FA-GW mixture with the cleaning solution, some changes in the IR spectrum of the stabilized material were noted. The cleaning solution, being highly alkaline (pH between 12 and 14), attacks the amorphous acid oxides included in the precursor materials (FA and GW), and even oxides such as  $\text{FeO}$  and  $\text{Fe}_2\text{O}_3$  can be affected by the alkaline attack (Lemoungna et al., 2013; Lloyd et al., 2009; van Deventer et al., 2007). Some signals are preserved, such as those from the crystalline quartz 455  $\text{cm}^{-1}$ .

On the other hand, bands around 643 and 689  $\text{cm}^{-1}$  can be attributed to new reaction products. According to Criado et al. (2007), in the region between 500 and 800  $\text{cm}^{-1}$  the typical signals of various cyclic structures of aluminosilicates formed by the union of  $\text{SiO}_4$  and  $\text{AlO}_4$  tetrahedra, linked by oxygen atoms resulting from the alkaline attack, are identified. The compounds identified in the cleaning solution apparently now form part of the new structure of the cementing gel, since the signals of the  $\text{Al}(\text{OH})_3$  aluminates and  $\text{AlO}_4$  tetrahedra are not noticeable in the new stabilized material, and even the signal identified as representing the  $\text{Al}=\text{O}$  link (1425  $\text{cm}^{-1}$ ) has significantly decreased. The main band of the stabilized material located around 967  $\text{cm}^{-1}$ , can represent different types of overlapping links and structures. Generally the

region between 950 and 1250  $\text{cm}^{-1}$  of the FTIR spectrum corresponds to  $\text{Si}-\text{O}-\text{T}$  type bonds ( $\text{T} = \text{Si}, \text{Al}$ ) which indicates that the main reaction product generated by the dissolution of the precursors is an aluminosilicate gel. This region is also related to signals from reactive terminals of the type  $\text{Si}-\text{O}-\text{Na}$  plus whichever ions are responsible for generating the aluminosilicate chains (Lee and Van Deventer, 2003). The precise location of the band in this region will depend on the type of generated structure, of alkaline activator used and of the composition of the binding gel (Criado et al., 2007).

### 3.4. SEM

The microstructure of the stabilized soil was examined with scanning electron microscopy, complemented with energy dispersive spectroscopy, for chemical assessment of the binding gel developed. Some of the images obtained (the analysis was performed on a sample collected from one of the previously tested CEBs) are presented in Fig. 11, showing the overall morphology of the stabilized soil (Fig. 11a), where the binding effect of the material synthesized from alkaline activated residues is clear, resulting in a homogeneous and fairly compacted structure with apparently well cemented soil particles. Fig. 11b presented the cemented soil particles in higher detail, where it is possible to detect both precursor and soil particles embedded in what appears to be the cementitious matrix. The nature of the reaction products was identified as a



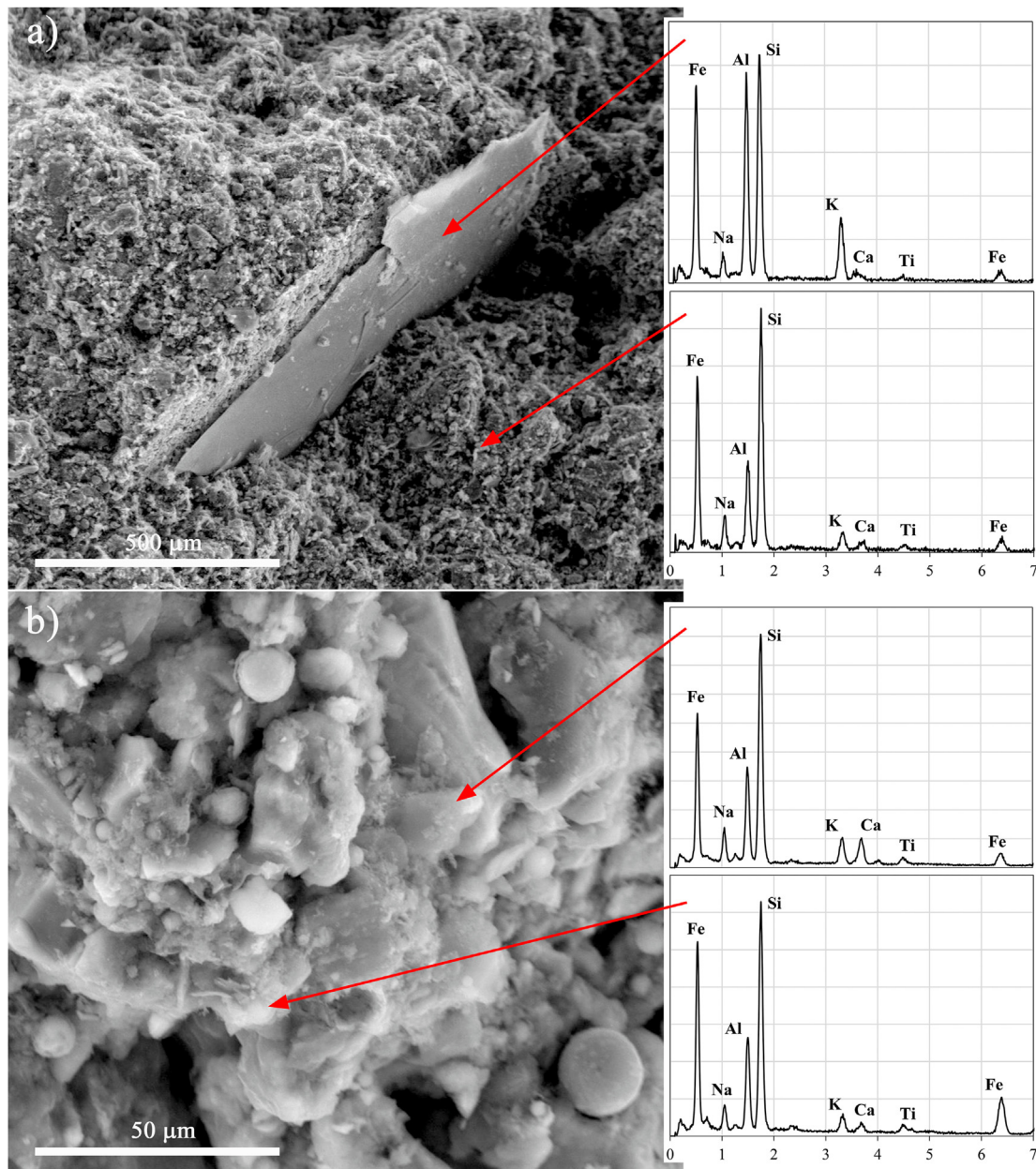


Fig. 11. SEM micrographs of the CEB structure.

sodium aluminosilicate gel (N-A-S-H), which corroborates the characterization done with FTIR. Indeed, it was previously proposed that the nature of the reaction products was a sodium aluminosilicate gel, due to the nature of the precursors and the alkaline activator.

#### 4. Conclusions

This research work demonstrated the viability of alternative and environmentally friendly soil stabilisation, with the specific purpose of manufacturing masonry elements commonly known as “compressed earth blocks”, or CEBs. The alternative synthesized cements are 100% based on industrial waste, and its applicability to soil stabilisation was thoroughly assessed through strength and durability tests. The results showed that such material can be an effective alternative to traditional chemical stabilisation of soils,

namely to calcium-based cements, such as lime or Portland cement. The manufacture of compacted earth masonry elements using this type of cementitious material suggests both a technical and environmental advantage since, in theory, the amount of incorporated energy in waste-based binding agents is significantly lower than the energy associated with traditional binders. However, and in order to fully corroborate this, it will be necessary to perform a comparison between both types of binders, in order to characterised and make evident and all the advantages and disadvantages.

#### Funding

This work was funded by the R&D Project JUSTREST- Development of Alkali Binders for Geotechnical Applications Made Exclusively from Industrial Waste, with reference PTDC/ECM-GEO/0637/

2014, financed by the Foundation for Science and Technology - FCT/MCTES (PIDDAC).

The research was supported by the GEO-DESIGN project, nº17501, co-financed by the European Regional Development Fund (ERDF) through NORTE 2020 (North Regional Operational Program, 2014/2020).

### CRediT authorship contribution statement

**Jhonathan Rivera:** Methodology, Writing - original draft, Software. **João Coelho:** Data curation, Investigation. **Rui Silva:** Investigation, Resources. **Tiago Miranda:** Visualization, Resources. **Fernando Castro:** Validation, Funding acquisition.

### Declaration of competing interest

The authors declare that they have no known competing financial interests or personal relationships that could have appeared to influence the work reported in this paper.

### Acknowledgments

The authors would also like to acknowledge the contribution of the Electronic Microscopy Unit of the University of Trás-os-Montes e Alto Douro (Dr. Lisete Fernandes), for the microstructural analysis.

### References

- ASTM C618, 2012. Standard specification for coal fly ash and raw or calcined natural pozzolan for use in concrete. ASTM Int. Annu. B. Stand. 1–5.
- ASTM C62-17, 2017. Standard Specification for Building Brick (Solid Masonry Units Made From Clay or Shale). ASTM International, West Conshohocken, PA. [www.astm.org](http://www.astm.org).
- Avila-López, U., Almanza-Robles, J.M., Escalante-García, J.L., 2015. Investigation of novel waste glass and limestone binders using statistical methods. *Construct. Build. Mater.* 82, 296–303.
- Bakharev, T., 2005. Geopolymeric materials prepared using Class F fly ash and elevated temperature curing. *Cement Concr. Res.* 35, 1224–1232.
- Corrêa-Silva, M., Araújo, N., Cristelo, N., Miranda, T., Gomes, A.T., Coelho, J., 2019. Improvement of a clayey soil with alkali activated low-calcium fly ash for transport infrastructures applications. *Road Mater. Pavement Des.* 20, 1912–1926.
- Criado, M., Fernández-Jiménez, A., Palomo, A., 2007. Alkali activation of fly ash: effect of the SiO<sub>2</sub>/Na<sub>2</sub>O ratio. *Microporous Mesoporous Mater.* 106, 180–191.
- Criado, M., Fernández-Jiménez, A., Palomo, A., 2010. Alkali activation of fly ash. Part III: effect of curing conditions on reaction and its graphical description. *Fuel* 89, 3185–3192.
- Cristelo, N., Fernández-Jiménez, A., Castro, F., Fernandes, L., Tavares, P., 2019. Sustainable alkaline activation of fly ash, aluminium anodising sludge and glass powder blends with a recycled alkaline cleaning solution. *Construct. Build. Mater.* 204, 609–620.
- Cristelo, N., Fernández-Jiménez, A., Vieira, C., Miranda, T., Palomo, Á., 2018. Stabilisation of construction and demolition waste with a high fines content using alkali activated fly ash. *Construct. Build. Mater.* 170, 26–39.
- DIN 18945-47, 2013. Earth Blocks - Terms, Requirements, Test Methods. DIN Stand.
- El-Mahllawy, M.S., Kandeel, A.M., Latif, M.L.A., El Nagar, A.M., 2018. The feasibility of using marble cutting waste in a sustainable building clay industry. *Recycling* 3, 39.
- Espinoza, L.J., Escalante García, I., 1970. Morteros a base de vidrio de desecho/escoria de alto horno; activación mecanoquímica del vidrio en soluciones alcalinas. *Nexo Rev. Científica* 24, 92–103.
- Fernandes, J., Peixoto, M., Mateus, R., Gervásio, H., 2019. Life cycle analysis of environmental impacts of earthen materials in the Portuguese context: rammed earth and compressed earth blocks. *J. Clean. Prod.* 241.
- Fernández-Jiménez, A., Cristelo, N., Miranda, T., Palomo, Á., 2017. Sustainable alkali activated materials: precursor and activator derived from industrial wastes. *J. Clean. Prod.* 162, 1200–1209.
- Fernández-Jiménez, A., Monzó, M., Vicent, M., Barba, A., Palomo, A., 2008. Alkaline activation of metakaolin-fly ash mixtures: obtain of Zeoceramics and Zeocements. *Microporous Mesoporous Mater.* 108, 41–49.
- Fernández-Jiménez, A., Palomo, A., Sobrados, I., Sanz, J., 2006. The role played by the reactive alumina content in the alkaline activation of fly ashes. *Microporous Mesoporous Mater.* 91, 111–119.
- Gao, K., Lin, K.L., Wang, D., Hwang, C.L., Shiu, H.S., Chang, Y.M., Cheng, T.W., 2014. Effects SiO<sub>2</sub>/Na<sub>2</sub>O molar ratio on mechanical properties and the microstructure of nano-SiO<sub>2</sub> metakaolin-based geopolymers. *Construct. Build. Mater.* 53, 503–510.
- Horpibulsuk, S., Rachan, R., Raksachon, Y., 2009. Role of fly ash on strength and microstructure development in blended cement stabilized silty clay. *Soils Found.* 49, 85–98.
- Houben, H., Guillaud, H., 1994. *Earth Construction: a Comprehensive Guide*. Intermediate Technology Publications.
- Hwang, J.-Y., Huang, X., Garkida, A., Hein, A., 2006. Waste colored glasses as sintering aid in ceramic tiles production. *J. Miner. Mater. Char. Eng.* 5, 119–129.
- Jamshidi, A., Nikudel, M.R., Khomehchiyan, M., 2016. Evaluation of the durability of Gerdooe travertine after freeze-thaw cycles in fresh water and sodium sulfate solution by decay function models. *Eng. Geol.* 202, 36–43.
- Kaufhold, S., Hein, M., Dohrmann, R., Ufer, K., 2012. Quantification of the mineralogical composition of clays using FTIR spectroscopy. *Vib. Spectrosc.* 59, 29–39.
- Khalil, E.M.A., ElBatal, F.H., Hamdy, Y.M., Zidan, H.M., Aziz, M.S., Abdelghany, A.M., 2010. Infrared absorption spectra of transition metals-doped soda lime silica glasses. *Phys. B Condens. Matter* 405, 1294–1300.
- Lee, W.K.W., Van Deventer, J.S.J., 2003. Use of infrared spectroscopy to study geopolymerization of heterogeneous amorphous aluminosilicates. *Langmuir* 19, 8726–8734.
- Leitão, D., Barbosa, J., Soares, E., Miranda, T., Cristelo, N., Briga-Sá, A., 2017. Thermal performance assessment of masonry made of ICEB's stabilised with alkali-activated fly ash. *Energy Build.* 139, 44–52.
- Lemoungna, P.N., MacKenzie, K.J.D., Jameson, G.N.L., Rahier, H., Chinje Melo, U.F., 2013. The role of iron in the formation of inorganic polymers (geopolymers) from volcanic ash: a <sup>57</sup>Fe Mössbauer spectroscopy study. *J. Mater. Sci.* 48, 5280–5286.
- Li, X., Bin, Zhao, D.F., Yang, S.S., Wang, D.Q., Zhou, Q.S., Liu, G.H., 2014. Influence of thermal history on conversion of aluminate species in sodium aluminate solution. *Trans. Nonferrous Met. Soc. China (English Ed.)* 24, 3348–3355.
- Lima, S.A., Varum, H., Sales, A., Neto, V.F., 2012. Analysis of the mechanical properties of compressed earth block masonry using the sugarcane bagasse ash. *Construct. Build. Mater.* 35, 829–837.
- Lin, K.L., Shiu, H.S., Shie, J.L., Cheng, T.W., Hwang, C.L., 2012. Effect of composition on characteristics of thin film transistor liquid crystal display (TFT-LCD) waste glass-metakaolin-based geopolymers. *Construct. Build. Mater.* 36, 501–507.
- Lloyd, R.R., Provis, J.L., Van Deventer, J.S.J., 2009. Microscopy and microanalysis of inorganic polymer cements. 1: remnant fly ash particles. *J. Mater. Sci.* 44, 608–619.
- MA, S. hua, ZHENG, S. li, XU, bin, H., Zhang, Y., 2007. Spectra of sodium aluminate solutions. *Trans. Nonferrous Met. Soc. China (English Ed.)* 17, 853–857.
- Mak, K., MacDougall, C., Fam, A., 2016. Freeze-thaw performance of on-site manufactured compressed earth blocks: effect of water repellent and other additives. *J. Mater. Civ. Eng.* 28, 04016034.
- Miranda, T., Leitão, D., Oliveira, J., Corrêa-Silva, M., Araújo, N., Coelho, J., Fernández-Jiménez, A., Cristelo, N., 2020. Application of alkali-activated industrial wastes for the stabilisation of a full-scale (sub)base layer. *J. Clean. Prod.* 242, 118427.
- Miranda, T., Silva, R.A., Oliveira, D.V., Leitão, D., Cristelo, N., Oliveira, J., Soares, E., 2017. ICEBs stabilised with alkali-activated fly ash as a renewed approach for green building: exploitation of the masonry mechanical performance. *Construct. Build. Mater.* 155, 65–78.
- Montgomery, D.C., Runger, G.C., 2014. *Applied Statistics and Probability for Engineers*, sixth ed. Blood Pressure.
- Narayanaswamy, A.H., Walker, P., Venkatarama Reddy, B.V., Heath, A., Maskell, D., 2020. Mechanical and thermal properties, and comparative life-cycle impacts, of stabilised earth building products. *Construct. Build. Mater.* 243, 118096.
- Nayak, P.S., Singh, B.K., 2007. Instrumental characterization of clay by FTIR, XRF, BET and, TPD-NH<sub>3</sub>. *Bull. Mater. Sci.* 30, 235–238.
- Novais, R.M., Ascensão, G., Seabra, M.P., Labrincha, J.A., 2016. Waste glass from end-of-life fluorescent lamps as raw material in geopolymers. *Waste Manag.* 52, 245–255.
- Olufowobi, J., Ogundoku, A., Michael, B., Aderinlewo, O., 2014. Clay soil stabilisation using powdered glass. *J. Eng. Sci. Technol.* 9, 541–558.
- Omar, Sore, S., Messan, A., Prud'homme, E., Escadeillas, G., Tsobnang, F., 2018. Stabilization of compressed earth blocks (CEBs) by geopolymer binder based on local materials from Burkina Faso. *Construct. Build. Mater.* 165, 333–345.
- Oti, J.E., Kinuthia, J.M., Bai, J., 2009a. Compressive strength and microstructural analysis of unfired clay masonry bricks. *Eng. Geol.* 109, 230–240.
- Oti, J.E., Kinuthia, J.M., Bai, J., 2009b. Engineering properties of unfired clay masonry bricks. *Eng. Geol.* 107, 130–139.
- Pacheco-Torgal, F., Jalali, S., 2012. *Earth construction: Lessons from the past for future eco-efficient construction*. *Construct. Build. Mater.* 29, 512–519.
- Panias, D., Giannopoulou, I.P., Perraki, T., 2007. Effect of synthesis parameters on the mechanical properties of fly ash-based geopolymers. *Colloids Surfaces A Physicochem. Eng. Asp.* 301, 246–254.
- Pascual, A.B., Tognonvi, M.T., Tagnit-hamou, A., 2014. Waste glass powder-based alkali-activated mortar. *Int. J. Res. Eng. Technol.* 3, 32–36.
- Preethi, R.K., Venkatarama Reddy, B.V., 2020. Experimental investigations on geopolymer stabilised compressed earth products. *Construct. Build. Mater.* 257, 119563.
- Ram, S., 2001. Infrared spectral study of molecular vibrations in amorphous, nanocrystalline and AlO(OH) · xH<sub>2</sub>O bulk crystals. *Infrared Phys. Technol.* 42, 547–560.
- Rios, S., Cristelo, N., da Fonseca, A.V., Ferreira, C., 2016. Structural performance of alkali-activated soil ash versus soil cement. *J. Mater. Civ. Eng.* 28.
- Rivera, J.F., Cristelo, N., Fernández-Jiménez, A., Mejía de Gutiérrez, R., 2019.



- Synthesis of alkaline cements based on fly ash and metallurgic slag: optimization of the  $\text{SiO}_2/\text{Al}_2\text{O}_3$  and  $\text{Na}_2\text{O}/\text{SiO}_2$  molar ratios using the response surface methodology. *Construct. Build. Mater.* 213, 424–433.
- Rivera, J.F., Cuarán-Cuarán, Z.I., Vanegas-Bonilla, N., Mejía de Gutiérrez, R., 2018. Novel use of waste glass powder: production of geopolymeric tiles. *Adv. Powder Technol.* 29, 3448–3454.
- Rivera, J.F., Mejía de Gutiérrez, R., Ramirez-Benavides, S., Orobio, A., 2020. Compressed and stabilized soil blocks with fly ash-based alkali-activated cements. *Construct. Build. Mater.* 264, 120285.
- Ryu, G.S., Kim, S.H., Koh, K.T., Kang, S.T., Lee, J.H., 2012. Influence of curing temperature on the mechanical properties of alkali-activated bottom ash geopolymer mortar. In: *Key Engineering Materials*, pp. 198–201.
- Saeli, M., Micale, R., Seabra, M.P., Labrincha, J.A., La Scalia, G., 2020. Selection of novel geopolymeric mortars for sustainable construction applications using Fuzzy topsis approach. *Sustainability* 12, 5987.
- Saeli, M., Tobaldi, D.M., Seabra, M.P., Labrincha, J.A., 2019. Mix design and mechanical performance of geopolymeric binders and mortars using biomass fly ash and alkaline effluent from paper-pulp industry. *J. Clean. Prod.* 208, 1188–1197.
- Saikia, B.J., Parthasarathy, G., 2010. Fourier Transform infrared spectroscopic characterization of kaolinite from Assam and Meghalaya, northeastern India. *J. Mod. Phys.* 1, 206–210.
- Schroeder, H., 2016a. The development of earth building. In: *Sustainable Building with Earth*. Springer International Publishing, Cham, pp. 1–46.
- Schroeder, H., 2016b. *Sustainable Building with Earth*. Springer International Publishing, Cham.
- Sekhar, D., Nayak, S., 2018. Utilization of granulated blast furnace slag and cement in the manufacture of compressed stabilized earth blocks. *Construct. Build. Mater.* 166, 531–536.
- Shakir, A.A., Wan Ibrahim, M.H., Othman, N.H., Ahmed Mohammed, A., Burhanudin, M.K., 2020. Production of eco-friendly hybrid blocks. *Construct. Build. Mater.* 257, 119536.
- Shoukry, H., 2019. Development of nano modified eco-friendly green binders for sustainable construction applications. *Nano Hybrids Compos* 24, 25–36.
- Siddiqua, S., Barreto, P.N.M., 2018. Chemical stabilization of rammed earth using calcium carbide residue and fly ash. *Construct. Build. Mater.* 169, 364–371.
- Silva, R. a, Soares, E., Oliveira, D.V., Miranda, T., Cristelo, N., Leitão, D., 2015. Mechanical characterisation of dry-stack masonry made of CEBs stabilised with alkaline activation. *Construct. Build. Mater.* 75, 349–358.
- Simonová, H., Keršner, Z., Schmid, P., Rovnaníková, P., 2018. Effect of curing temperature on mechanical and fracture parameters of alkali-activated brick powder based composite. In: *Key Engineering Materials*, pp. 79–82.
- Singh, G.V.P.B., Subramaniam, K.V.L., 2019. Influence of processing temperature on the reaction product and strength gain in alkali-activated fly ash. *Cement Concr. Compos.* 95, 10–18.
- Singh, S.K., Singh, A., Singh, B., Vashistha, P., 2020. Application of thermo-chemically activated lime sludge in production of sustainable low clinker cementitious binders. *J. Clean. Prod.* 264, 121570.
- Tarte, P., 1967. Infra-red spectra of inorganic aluminates and characteristic vibrational frequencies of  $\text{AlO}_4$  tetrahedra and  $\text{AlO}_6$  octahedra. *Spectrochim. Acta* 23A, 2127–2143.
- Torres-Carrasco, M., Palomo, J.G., Puertas, F., 2014. Sodium silicate solutions from dissolution of glasswastes. Statistical analysis. *Mater. Constr.* 64, e014.
- Torres-Carrasco, M., Puertas, F., 2015. Waste glass in the geopolymer preparation. Mechanical and microstructural characterisation. *J. Clean. Prod.* 90, 397–408.
- UNE41410, 2008. UNE 41410:2008 - Bloques de tierra comprimida para muros y taboques/Definiciones, especificaciones y métodos de ensayo. AENOR - Asoc. Española Norm. y Certificación 28.
- van Deventer, J.S.J., Provis, J.L., Duxson, P., Lukey, G.C., 2007. Reaction mechanisms in the geopolymeric conversion of inorganic waste to useful products. *J. Hazard Mater.* 139, 506–513.
- Varma, R.S., Kothari, D.C., Tewari, R., 2009. Nano-composite soda lime silicate glass prepared using silver ion exchange. *J. Non-Cryst. Solids* 355, 1246–1251.
- Véron, O., Blondeau, J.P., Meneses, D.D.S., Vignolle, C.A., 2013. Characterization of silver or copper nanoparticles embedded in Soda-lime glass after a staining process. *Surf. Coating Technol.* 227, 48–57.
- Zhang, Z., Wong, Y.C., Arulrajah, A., Horpibulsuk, S., 2018. A review of studies on bricks using alternative materials and approaches. *Construct. Build. Mater.* 188, 1101–1118.